Mesp2: a novel mouse gene expressed in the presegmented mesoderm and essential for segmentation initiation

Yumiko Saga,[1,2,6] Naomi Hata,[1] Haruhiko Koseki,[3] and Makoto M. Taketo[1,4,5]

[1]Banyu Tsukuba Research Institute (Merck), Tsukuba, 300-26, Japan; [2]Center for Tsukuba Advanced Research Alliance (TARA), University of Tsukuba, Tsukuba, 305 Japan; [3]CREST and Biomedical Science, Chiba University School of Medicine, Chuo-ku, Chiba 260 Japan; [4]Department of Biomedical Genetics, Faculty of Pharmaceutical Sciences, University of Tokyo, Bunkyo-ku, 113 Japan

We isolated a novel bHLH protein gene *Mesp2* (for mesoderm posterior 2) that cross-hybridizes with *Mesp1* expressed in the early mouse mesoderm. *Mesp2* is expressed in the rostral presomitic mesoderm, but down-regulated immediately after the formation of the segmented somites. To determine the function of MesP2 protein (MesP2) in somitogenesis, we generated *Mesp2*-deficient mice by gene targeting. The homozygous *Mesp2* (−/−) mice died shortly after birth and had fused vertebral columns and dorsal root ganglia, with impaired sclerotomal polarity. The earliest defect in the homozygous embryos was a lack of segmented somites. Their disruption of the metameric features, altered expression of *Mox-1, Pax-1,* and *Dll1,* and lack of expression of *Notch1, Notch2,* and *FGFR1* suggested that MesP2 controls sclerotomal polarity by regulating the signaling systems mediated by notch–delta and FGF, which are essential for segmentation.

[*Key Words:* bHLH; somitogenesis; segmentation; sclerotomal polarity; notch–delta signaling]

Received March 28, 1997; revised version accepted May 28, 1997.

Somitogenesis in the mouse embryo begins with the recruitment of prospective mesodermal cells from the primitive streak or the tail bud to the caudal end of the presomitic mesoderm (Tam and Trainor 1994). The mesenchymal cells are organized into somitomeres in presomitic mesoderm, which can be visualized only under a scanning electron microscope (SEM) (Meier 1979). The transformation of somitomeres into somites is accompanied by two major changes in tissue architecture, compaction and epithelialization, which lead to the formation of segmented somites (Ostrovsky et al. 1988). The cells situated ventromedially in a somite differentiate into the sclerotome, which gives rise to cartilage. From the remainder of the somite, the dermomyotome arises and differentiates into muscle and dermis. The rostral and caudal halves of a somite are different in terms of the cell density of the sclerotome (Stern et al. 1986), neural crest cell colonization (Rickmann et al. 1985), and motor nerve innervation (Rickmann et al. 1985; Keynes and Stern 1988). Thus, somites are important units forming the fundamental structure of an animal's body. The mechanism of somitogenesis has been studied most extensively in the chick embryo, a model that allows many experimental manipulations such as transplantation, cell marking, and chick–quail chimera analysis. For example, it has been shown that the rostrocaudal axis of the somite has already been determined at the segmentation stage, preceding cell differentiation (Stern and Keynes 1986; Aoyama and Asamoto 1988). However, the precise molecular mechanism that establishes sclerotomal polarity remains to be determined. The mechanism in the mouse is expected to be similar to that in the chicken, although no direct experimental evidence has been presented so far.

In both the chick and the mouse, cell organization changes in the maturing somitomeres are correlated with the differential expression of cell adhesion molecules, extracellular matrix, growth factors and their receptors, and some transcription factors. Recent gene knockout experiments suggest that some genes are essential in somitogenesis. For example, mice deficient in fibroblast growth factor receptor-1 (*FGFR-1*) (Deng et al. 1994; Yamaguchi et al. 1994), *Notch1* (Swiatek et al. 1994; Conlon et al. 1995), *RBP-Jk* (Oka et al. 1995), and Delta-like gene 1 (*Dll1*), the mouse Delta homolog (Hrabe de Angelis et al. 1997), have been shown to have defective somitogenesis. Because *FGFR-1, Notch1,* and *Dll1* are expressed predominantly in the presomitic mesoderm, they are likely to participate in the early stages of somitogenesis (Yamaguchi et al. 1992; Bettenhausen

[5]Present address: Department of Biomedical Genetics, Faculty of Pharmaceutical Sciences, University of Tokyo, Bunkyo-ku, 113 Japan.
[6]Corresponding author. Present address: Cellular and Molecular Toxicology, National Institute of Health Science, Kamiyohga, Setagaya-ku, 158 Japan.
E-MAIL saga@nihs.go.jp; FAX 81-3-3700-9647.

et al. 1995; Williams et al. 1995), whereas *RBP-Jk* is a downstream gene in the Notch signaling pathway. The basic helix–loop–helix (bHLH) protein gene *Paraxis* is expressed in paraxial mesoderm and somites, and its disruption results in the failure of cellular epithelialization required for dermomyotome formation (Burgess et al. 1996). The roles of these genes in somite formation and their interactions remain to be investigated.

Recently, we isolated *Mesp1* (mesoderm posterior 1), a bHLH gene expressed in nascent mesodermal cells during mouse gastrulation (Saga et al. 1996). Many mesoderm-specific bHLH proteins have been identified using the recent yeast two-hybrid system (Quertermous et al. 1994). These tissue-specific HLH proteins play important roles in cell lineage determination and differentiation. Here, we report the isolation and characterization of *Mesp2*, a novel gene that has an almost identical bHLH motif to that of *Mesp1*. To investigate its function, we have produced *Mesp2* (−/−) mice, which exhibit severe skeletal malformations attributable to a failure of segmentation.

Results

Mesp2 *is expressed transiently in the rostral part of the presomitic mesoderm immediately before segmentation*

During the genomic library screening for the *Mesp1* gene, we isolated a novel gene (designated as *Mesp2* for mesoderm posterior 2) that strongly cross-hybridized with the *Mesp1* probe. Both *Mesp1* and *Mesp2* were found to be located on chromosome 7, head to head, and separated only by 23 kb (Fig. 1A; Saga et al. 1996).

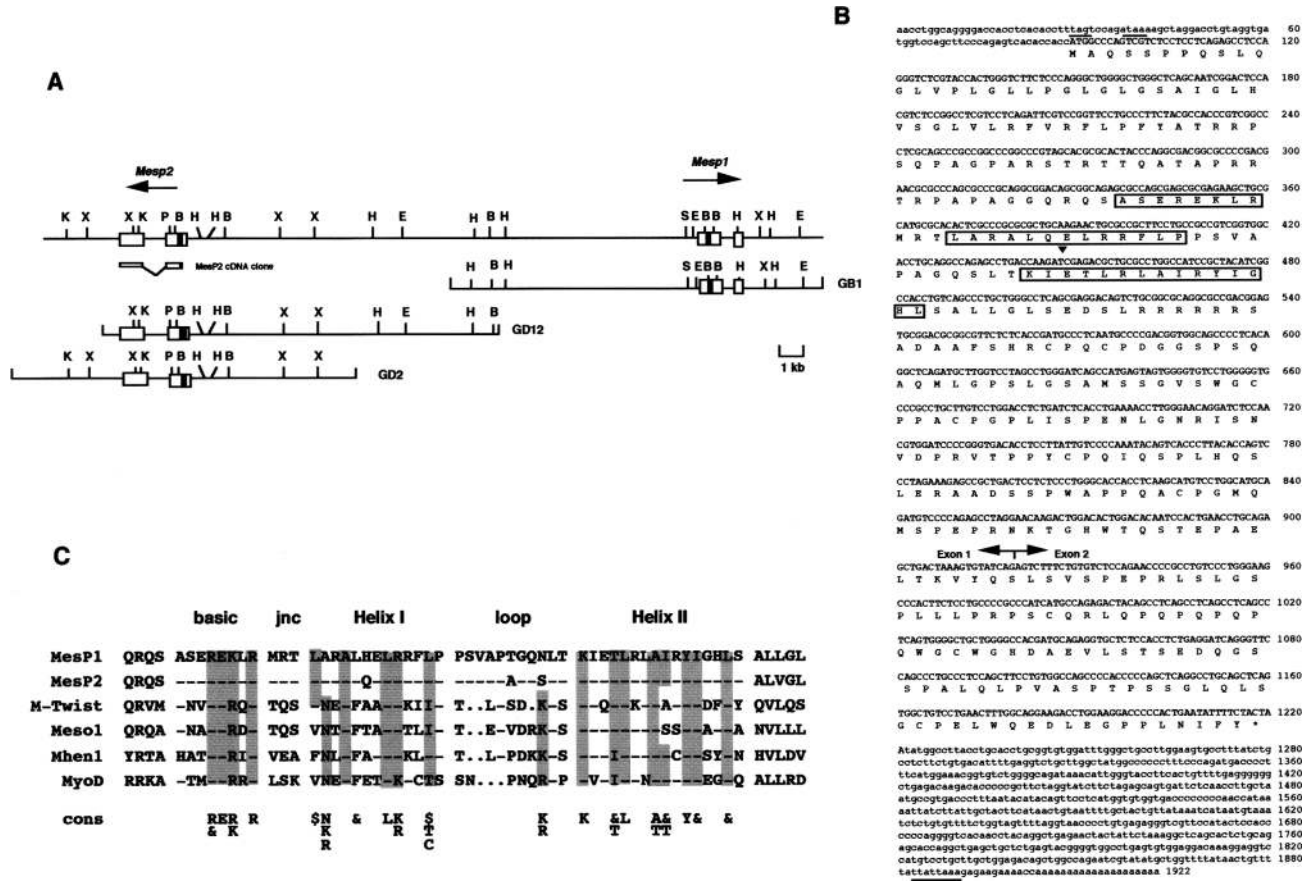

Figure 1. Cloning and sequence of the *Mesp2* gene. (*A*) Genomic organization of the *Mesp1* and *Mesp2* region, and the genomic phage clones that cover this region. The transcriptional orientation of each gene is indicated by an arrow. Exons are represented by open boxes and the bHLH regions are shown by solid boxes. (B) *Bam*HI; (E) *Eco*RI, (H) *Hin*dIII, (K) *Kpn*I, (P) *Pst*I, (S) *Sac*I, (X) *Xba*I. (*B*) Nucleotide and the deduced amino acid sequences of the *Mesp2* gene consolidated from those of the *Mesp2* cDNA clone, and a part of the genomic DNA (*A*). The sequence of intron 1 is not presented here. The 5′ end of the *Mesp2* cDNA clone is indicated as ▼. The amino acids corresponding to the bHLH motif are boxed. Two in-frame stop codons in the 5′ upstream region are underlined. The possible polyadenylation signal in the 3′ untranslated region is also underlined. (*C*) The bHLH motif in MesP1 and MesP2 are compared with those of other bHLH proteins, M-twist, meso-1 (also described as paraxis), HEN1, and MyoD. A hyphen indicates an identical amino acid. Shaded amino acids indicate residues that match the consensus (cons) derived from the known bHLH family (Cai and Davis 1990). ($) amino acids L, I, V, or M; (&) F, L, I, or Y.

Complementary DNA for *Mesp2* was isolated from 8.5-day postcoitus (dpc) embryo cDNAs (Fig. 1B). As shown in Figure 1C, *Mesp2* protein (MesP2) has an almost identical bHLH motif to that of MesP1 (93% amino acid identity), suggesting that these two genes form a novel bHLH subfamily.

As we described previously, initially *Mesp1* was expressed at the onset of gastrulation in 6.5- to 6.75-dpc embryos (Saga et al. 1996; Fig. 2A,B). Its expression was then down-regulated, and disappeared thereafter (Fig. 2C,D). Just before somitogenesis at 8.0 dpc, a pair of *Mesp1* bands reappeared on both sides of the node where somites are expected (Fig. 2E). In contrast to *Mesp1*, *Mesp2* expression was not detected in early stage embryos between 6.0 and 7.5 dpc. Interestingly, the earliest expression of *Mesp2* was found in 8.0-dpc embryos on both sides of the node at the same locations as for *Mesp1* expression (Fig. 2G). The in situ signals for both *Mesp1* and *Mesp2* were restricted to the rostral part of the presomitic mesoderm, but were absent in the newly formed somites (Fig. 2F,H–Q). The transcription of these genes ceased once the somite was formed from the presomitic mesodem. Usually, there was a one-somite-width space between the newly segmented somite and the *Mesp2*-expressing domain (Fig. 2I,J). The expression domain at the developmental stage 9.0–9.5 dpc was greater than that of earlier (8.0–8.5 dpc) or later (10.5–12.5 dpc) stages. Thus, sharper bands of in situ staining were observed during tail development (Fig. 2K–Q). This expression at the presomitic mesoderm continued until 12.5 dpc (Fig. 2Q) and disappeared before 13.5 dpc. These results suggest that MesP2 plays an important role in somitogenesis.

Homozygous Mesp2 *(-/-) mice show caudal truncation and severe skeletal malformations*

To investigate the function of MesP2 in somitogenesis, we constructed two independent *Mesp2*-deficient mouse strains with identical phenotypes (Fig. 3; see Materials

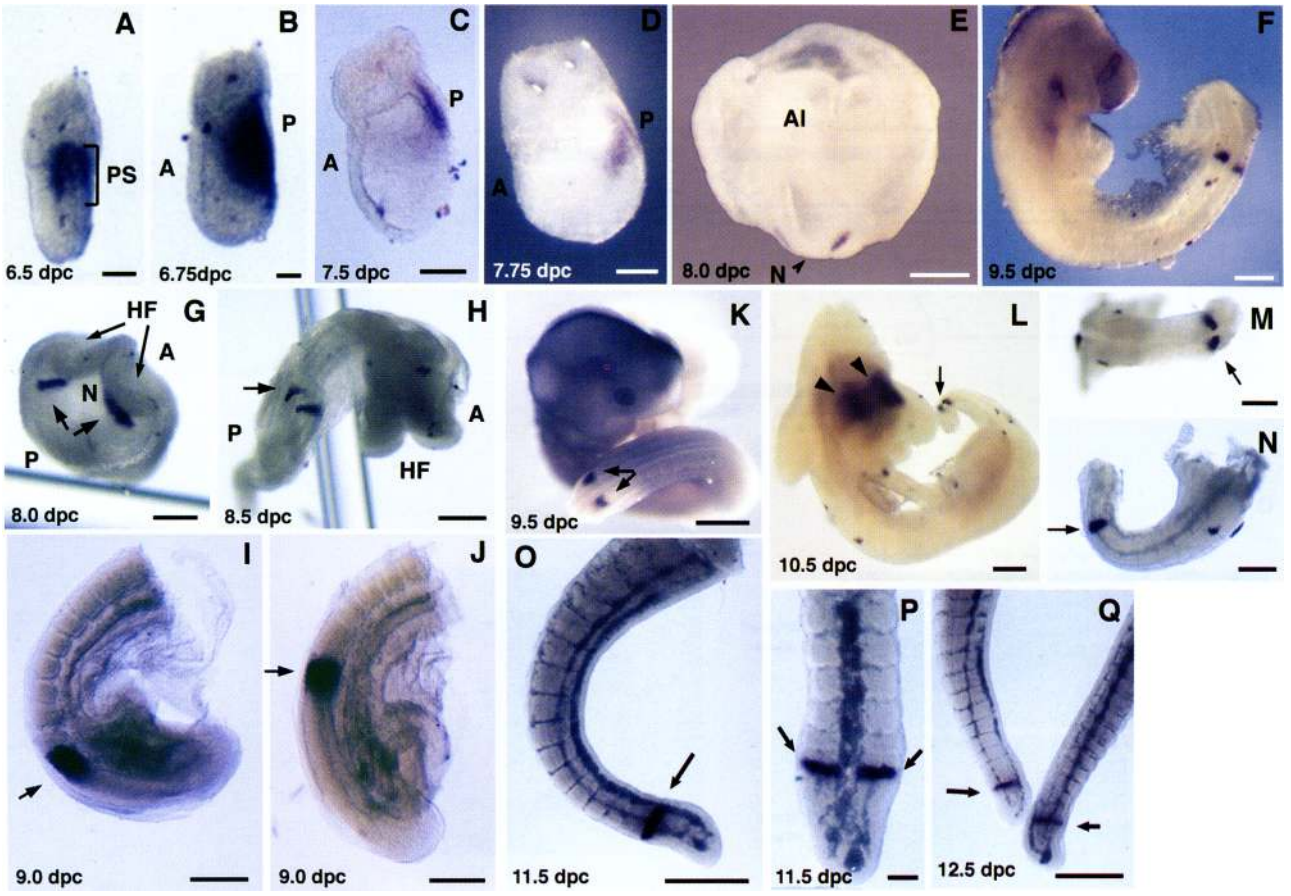

Figure 2. Expression of *Mesp2* mRNA detected by whole mount in situ hybridization and the comparison with *Mesp1* expression. (*A–F*) *Mesp1* expression observed at 6.5 dpc (*A*), 6.75 dpc (*B*) 7.5 dpc–7.75 (*C,D*), 8.0 dpc (*E*; posterior view), and 9.5 dpc (*F*). *Mesp2* expression was indicated by arrows at 8.0 dpc (*G*; ventral view); 8.5 dpc, (*H*) 9.0 dpc (*I,J*), 9.5 dpc (*K*), 10.5 dpc (*L–N*), 11.5 dpc (*O,P*), and 12.5 dpc (*Q*). *M* and *P* show magnified dorsal views of the tail portion of *L* and *O*, respectively. *N* is a lateral view of *L*. The staining in the thoracic region (arrowheads in *L*) was the result of nonspecific staining. (A) anterior; (Al) allantois; (HF) head fold, (N) node; (P) posterior; (PS) primitive streak. (*A,B,G,M,N,P*) Bars, 100 μm; (*H*) bar, 200 μm; (*C–E*) bar, 300 μm; (*K,L*) bar, 400 μm; (*F,I,J,O,Q*) bar, 500 μm.

and Methods). The F_1 *Mesp2* (+/−) mice were viable, fertile, and appeared normal. Heterozygous intercrosses yielded *Mesp2* (−/−) pups in the Mendelian ratio (Table 1). However, these mutant pups had short and tapered trunks with rudimentary tails (Fig. 3D). They died within 20 min after birth, although they could breathe several times and were mobile in response to mild pinches.

The abnormal external morphology of the *Mesp2* (−/−) mice was attributable mainly to severe skeletal malformations of the vertebral column (Fig. 4A,B). The metameric architecture of the vertebrae and ribs was markedly impaired along the entire axis (Fig. 4B,C); pedicles of neural arches, transverse processes of the lumbar vertebrae, and the proximal regions of the ribs were fused together (Fig. 4D). Thus, the segmentation of the lateral structures of the vertebrae was totally lost in the *Mesp2* (−/−) mutants (Fig. 4H). Although the vertebral bodies appeared to be amorphous, alignment of the ossification centers was irregular and intervertebral discs could not be identified clearly (Fig. 4G), segmentation of the ventral structures of each vertebra and the most proximal region of the rib was weakly retained (Fig. 4B,G). The dorsal structures of the vertebrae were affected to vari-

Table 1. *Genotype analysis of* Mesp2 *(+/−) intercross progeny*

Age (dpc)	+/+	+/−	−/−
9.5	15 (24.2%)	31 (50.0%)	16 (25.8%)
10.5	9 (24.3%)	13 (35.1%)	15 (40.5%)
11.5	12 (30.0%)	17 (42.5%)	11 (27.5%)
12.5–15.5	18 (36.0%)	24 (48.0%)	8 (16.0%)
18.5	12 (25.0%)	21 (43.7%)	15 (31.3%)
Subtotal	66 (27.8%)	106 (44.7%)	65 (27.4%)
3 weeks	46 (33.0%)	81 (66.9%)	0 (0%)

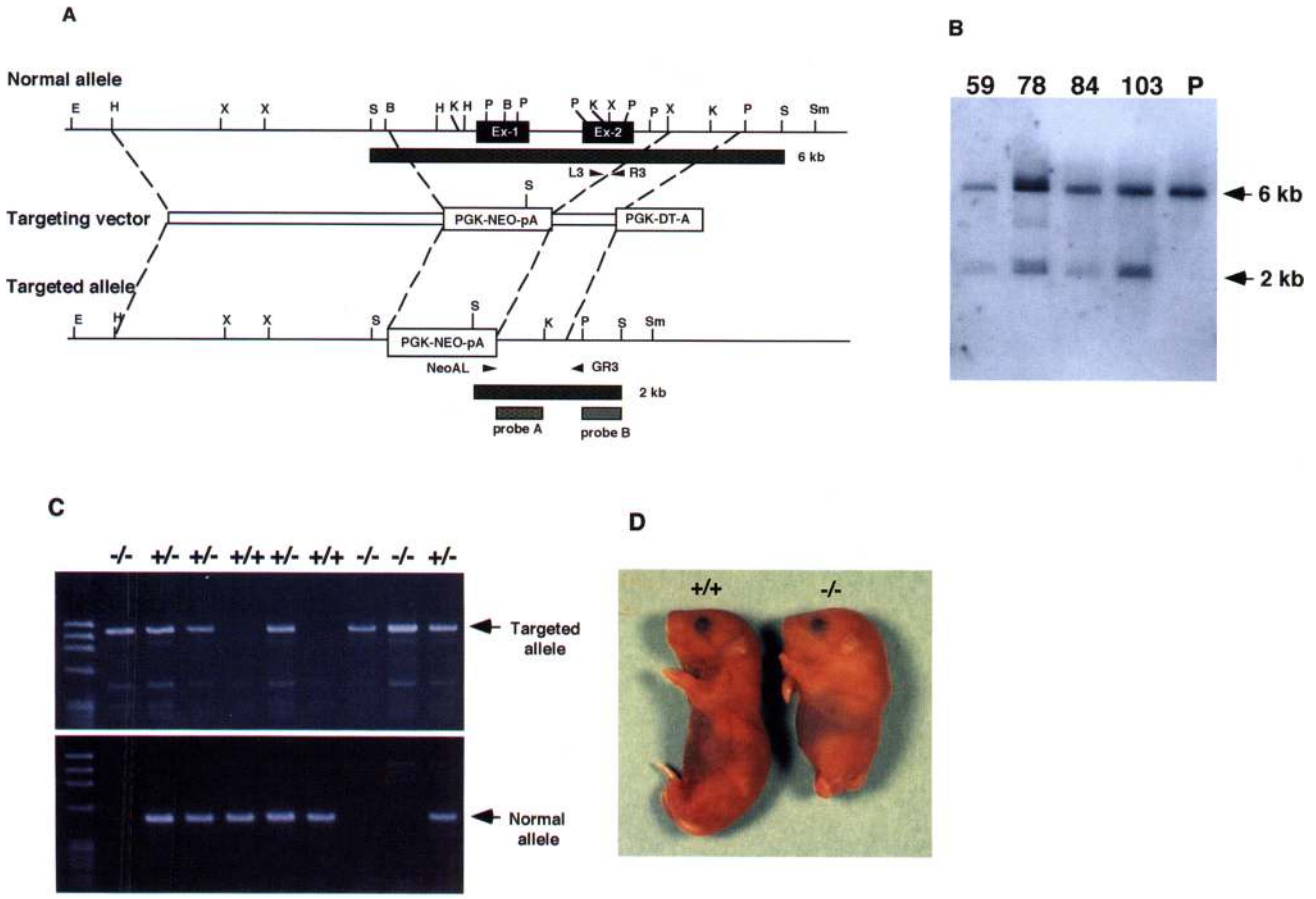

Figure 3. Targeted mutation in the *Mesp2* locus. (*A*) Schematic representation of the targeting strategy. Black boxes represent *Mesp2* exons. Primers, NeoAL and GR3 for the targeted allele and L3 and R3 for the normal allele are indicated by arrowheads. Probes A and B used for the Southern blot analysis are depicted by thick lines. (B) *Bam*HI; (E) *Eco*RI; (H) *Hin*dIII; (K) *Kpn*I; (P) *Pst*I; (S) *Sac*I; (Sm) *Sma*I; (X) *Xba*I. (*B*) Genomic Southern blot analysis of DNA from PCR-positive candidate ES cell clones. Probe A was used here. Arrows indicate the 2.0-kb *Sac*I fragment of the mutant allele compared with the wild-type 6.0-kb fragment. (P) Parental TT2 ES cell. (*C*) PCR determination of the genotypes of 8.5-dpc F_2 embryos. Yolk sac DNA was used for PCR. Their genotypes are indicated as +/+, +/−, or −/− (*top*). (*D*) Morphology of a *Mesp2* (−/−) mutant at birth compared with a wild-type littermate.

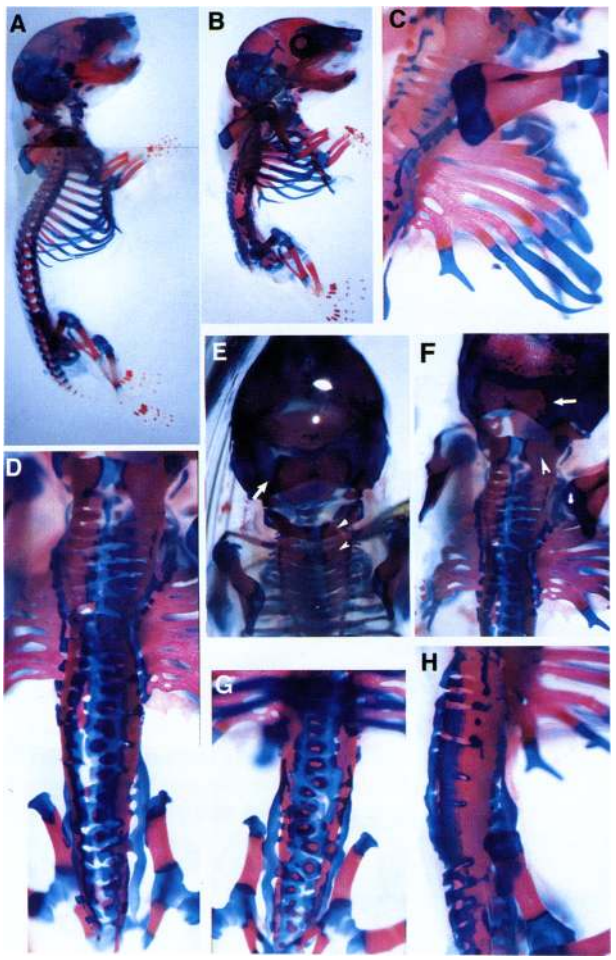

Figure 4. Skeletal anomalies observed in *Mesp2* (−/−) mutant mice. Wild-type (*A*) and mutant (*B*) newborn mice were stained for the bone and cartilage. Mutant ribs were fused in the proximal region (*C*). Vertebral column of the *Mesp2* (−/−) mutant, photographed from dorsal (*D*), ventral (*G*), or lateral (*H*) views. The occipital bone was formed normally in the mutant (*F*, arrows) as in the wild type (*E*); however, the atlas and axis (*E*, arrowheads) were completely fused in the mutant (*F*, arrowhead).

able extents along the anteroposterior axis (Fig. 4D). In the lumbosacral region, the laminae of the vertebral arches were not formed, resulting in spina bifida (Fig. 4H). These results indicate that segmentation of the somitic mesoderm is severely, but not completely, impaired in *Mesp2* (−/−) mutants. Because the pedicles of the neural arches are derived from the caudal half of the somite (Goldstein and Kalcheim 1992), the sclerotome of *Mesp2* (−/−) mutants may lack the properties of the rostral half.

It is worth noting that joint formation between the occipital bone and the atlas was not affected in the *Mesp2* (−/−) mice (Fig. 4E,F), although the atlas and axis were always fused in *Mesp2* (−/−) mutants. In contrast to the skeletal system, no particular abnormalities were found in the dermis or muscles of these mutants. Histological pictures of the muscle fiber alignment were indistinguishable between *Mesp2* (−/−) mice and their (+/−) or (+/+) littermates (data not shown).

Lack of segmentation appears to be the primary defect in Mesp2 *(−/−) embryos*

To determine the initial defect in the *Mesp2* (−/−) mice, we investigated intercross embryos at various stages of development. *Mesp2* (−/−) embryos could not be distinguished easily from their sibs at 8.0–8.5 dpc just after the initiation of somitogenesis (Fig. 5A). The parasagittal sections revealed the presence of segmented somites (Fig. 5B). Accordingly, the several early somites in the presumptive occipitocervical region were generated at the appropriate timing. However, the defect of segmentation of the paraxial mesoderm became obvious externally in the presumptive cervicothoracic region of 9.0-dpc *Mesp2* (−/−) embryos, whereas the segmentation was apparent in the comparable level of the wild-type littermates (Fig. 5C). Histological examination of 9.5-dpc embryos again indicated the defective segmentation at the comparative position in *Mesp2* (−/−) embryos (Fig. 5D). In mutants, the differentiation of the somitic mesoderm into the dermomyotome and sclerotome occurred without segmentation of the paraxial mesoderm (indicated as DM in Fig. 5D). Interestingly, delayed and irregular segmentation was observed in the dermomyotome without obvious segmentation of the sclerotome in *Mesp2* (−/−) embryos. The defect in segmentation was most conspicuous in the caudal region of 11.5-dpc *Mesp2* (−/−) embryos, whereas the development of the dermomyotome and sclerotome was intact (Fig. 5E,F). Segmentation of the dermomyotome was apparent in the trunk region as seen in 10.5-dpc *Mesp2* (−/−) embryos (Fig. 6B; Y. Saga, unpubl.). In the caudal part of 12.5-dpc *Mesp2* (−/−) embryos, apparent but irregular segmentation was observed (Fig. 5G). Taken together, segmentation of the paraxial mesoderm was delayed significantly but not blocked completely in *Mesp2* (−/−) embryos, and was more severely affected in the sclerotome than the dermomyotome.

Segment polarity of the paraxial mesoderm was impaired in Mesp2 *(−/−) embryos*

As the establishment of the craniocaudal polarity in each somite is tightly correlated with the generation of the metameric appearance of the vertebral column, several histological parameters indicating the segment polarity of the sclerotome within each segment was investigated in 10.5-dpc *Mesp2* (−/−) embryos (Fig. 6). In the prospective cervicothoracic region of 10.5-dpc wild-type embryos, the sclerotome was divided into loose rostral and dense caudal parts (Fig. 6A,C, indicated as R and C, respectively, in Fig. 6C). In *Mesp2* (−/−) embryos, the defects of the sclerotome patterning were different along with the anteroposterior axis. At the prospective cervical region, no clear distinction was observed between rostral and caudal sclerotomal compartments although inter-

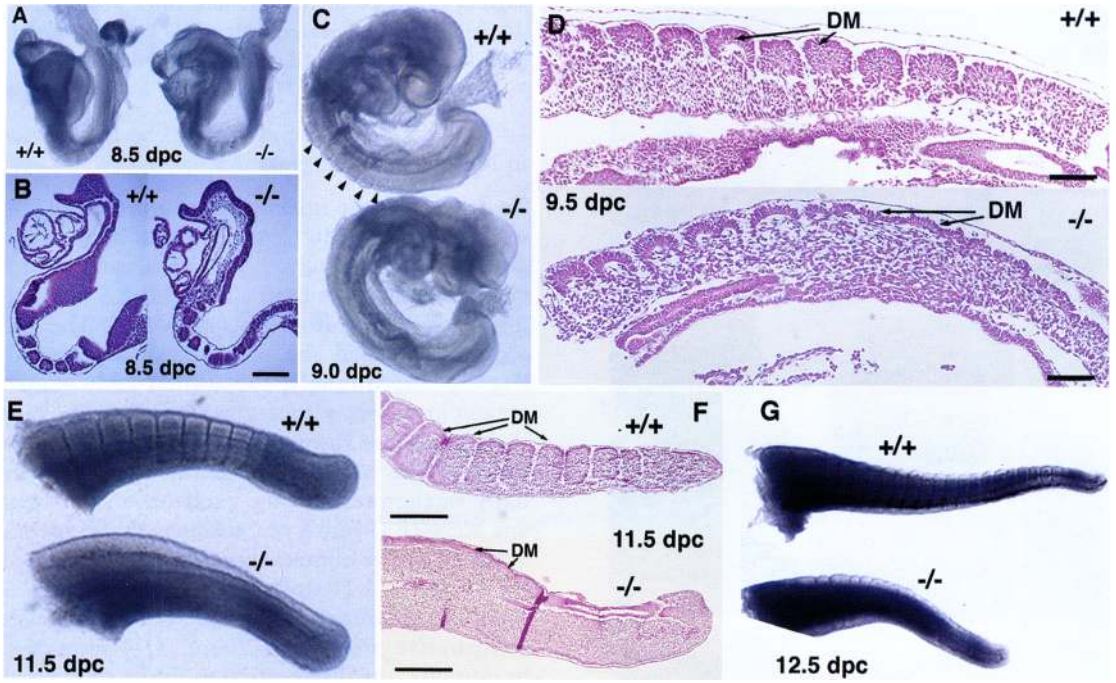

Figure 5. The *Mesp2* (−/−) embryo had defective segmentation. Segmented somites were observed in the *Mesp2* (−/−) embryo at 8.5 dpc (*A,B*), but clearly segmented blocks seen in the wild-type embryo (arrowheads in *C*) were not visible in the mutant at 9.0 dpc (*C*) or 11.5 dpc (*E*). Parasagittal section caudal region at 9.5 dpc (*D*) and 11.5 dpc (*F*) embryos revealed the defective abnormal somitogenesis in *Mesp2* (−/−) mutants. In the *Mesp2* (−/−) mutant, dermomyotome (DM) differentiation preceded without segmentation (*D,F*). (*G*) Segmentation of *Mesp2* (−/−) mutant at 12.5 dpc. (*B,D*) Bar, 200 μm; (*F*) bar, 400 μm.

somitic boundaries were generated in *Mesp2* (−/−) embryos (Fig. 6B,D). In the prospective thoracolumbar region of *Mesp2* (−/−) embryos, not only the craniocaudal polarity of each sclerotome, but also the boundary distinguishing each segment was unclear. Neural crest cells are known to migrate through the rostral half of the sclerotome to generate the dorsal root ganglion (DRG) and spinal nerve axons. It was apparently seen that spinal nerve axons passed through the rostral compartment of each sclerotome as reported previously (indicated as SN in Fig. 6C) (Stern and Keynes 1987). In the *Mesp2* (−/−) embryos, spinal nerve axons passed through the center of the sclerotome in the presumptive cervical region (Fig. 6B,D). In the prospective thoracolumbar region of *Mesp2* (−/−) embryos, a strong impairment of axonal outgrowth of spinal nerves into the ventral sclerotome was obvious by staining with neurofilament-specific monoclonal antibody 2H3, with the disturbed axons fused to each other (Fig. 6). Development of DRG was also affected in *Mesp2* (−/−) embryos, therefore, DRG did not show clear compartmentalization but fused and located dorsally compared to those of the wild type (Fig. 6F–J,L,M). The cranial nerves were not affected in *Mesp2* (−/−) embryos (Fig. 6J,L). These observations strongly suggest that the establishment of the segment polarity, particularly the rostral half properties of the sclerotome is strongly impaired in *Mesp2* (−/−) embryos.

To confirm and extend this interpretation, several molecular markers implicated in somitogenesis were investigated in *Mesp2* (−/−) mutants. *Mox-1* is expressed in the anterior presomitic mesoderm and in the somite (Candia et al. 1992). As shown in Figure 7A, its expression was higher in the caudal half of the somite in the wild-type embryos. In the *Mesp2* (−/−) embryos, diffuse staining was observed rather than a striated pattern. *Pax-1* is a caudal marker of the sclerotomal compartment (Koseki et al. 1993). Although the *Mesp2* (−/−) embryos expressed *Pax-1* strongly, its staining lacked the segmental pattern found in the wild-type embryos (Fig. 7B). *Paraxis* which encodes a bHLH protein, is expressed in the rostral part of the presomitic mesoderm and newly formed somite and, subsequently, localized to the dermomyotome and the dermatome (Burgess et al. 1995). Expression of *paraxis* in the *Mesp2* (−/−) embryos was detected in the right place, the prospective presomitic mesoderm or newly formed somite region, although there was no segmentaion. Later, it was expressed in the delayed and irregular but segmented dermatomal region as in the wild-type embryos (Fig. 7C). Myogenin (encoded by *Myog*) is a marker for early myotomal cell lineage (Edmondson and Olson 1989). *Mesp2* (−/−) embryos showed a segmental expression pattern similar to that of the wild-type embryos, although the stripes of its expression were shorter and irregular (Fig. 7D). Therefore, the segmentation and establishment of the segment polarity of the sclerotome were strongly impaired in the *Mesp2* (−/−) embryos, whereas the dermatome and myotome were developed segmentally. These results indicate that

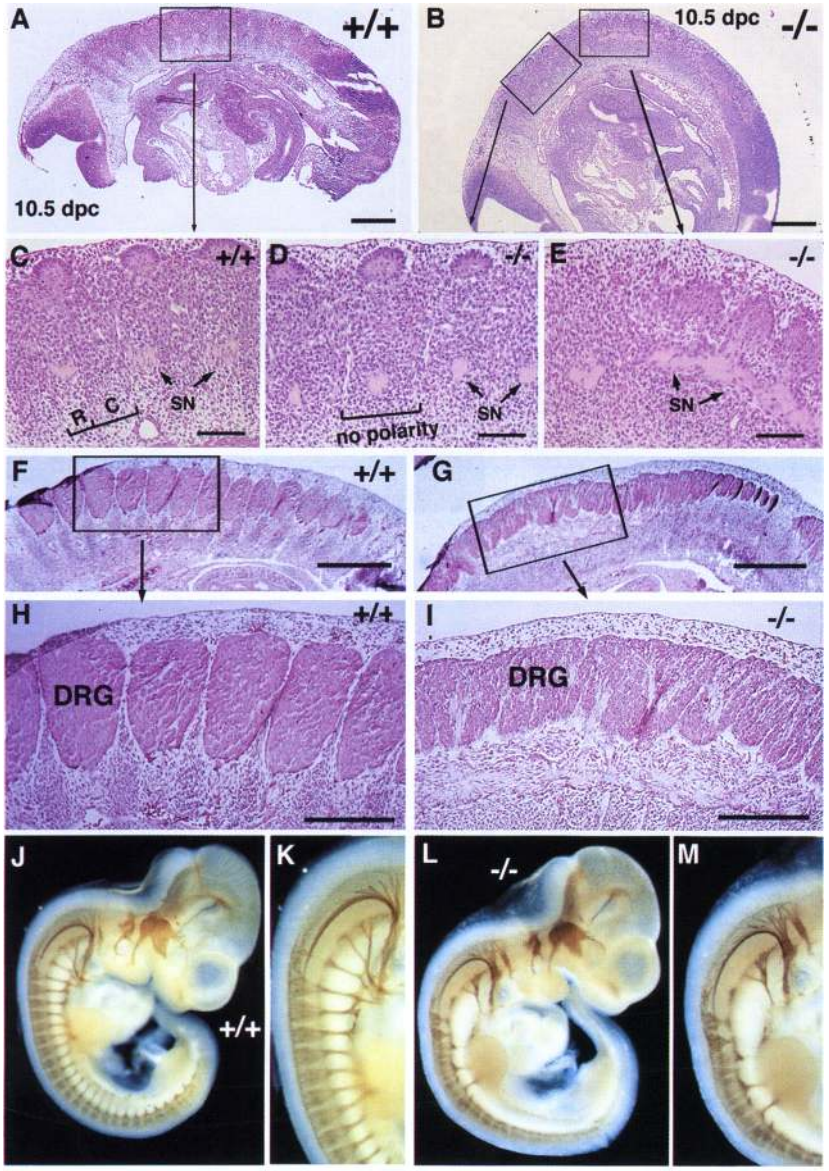

Figure 6. The *Mesp2* (−/−) embryo showed defective sclerotomal polarity and neuronal development. (*A–E*) Sclerotomal polarity represented by the difference in cell density in the wild-type embryo (*A,C*) did not exist in the *Mesp2* (−/−) embryo at 10.5 dpc (*B,D,E*). The magnified regions are indicated by rectangles. Spinal nerves (SN) were observed in the rostral part in the wild-type embryo (*C*), whereas they were located in the center at the cervical region (*D*) or fused at the thoracic region (*E*) in the mutant embryo. (*F–I*) Sections of the trunk region showing the development of DRG in an 11.5-dpc embryo. Fused and smaller DRG were located dorsally in the *Mesp2* (−/−) embryo (*G,I*), in contrast to the segmented large DRG observed in the wild-type embryo (*F,H*). (*J–M*) Neuronal axon development in 10.5-dpc embryos visualized by staining with monoclonal antibody 2H3. *K* and *M* are a higher magnification of *J* and *M*, respectively. No defect in the cranial nerves was seen in the *Mesp2* (−/−) mutant, whereas the spinal nerve showed defective development. (*A,B,F,G*) Bars, 400 μm; (*C,D,E,H,I* bar, 200 μm.

MesP2 is essentially required for the segmentation of the somite at an appropriate timing, and the establishment of the segment polarity of the sclerotome.

Mesp2 *(−/−) embryos lack sclerotomal polarity, probably because of defective notch–delta and FGF signaling pathway*

Because the phenotype was likely attributable to the lack of *Mesp2* expression at an early stage of segmentation, we determined the expression of genes involved in the transition from presomitic mesoderm to segmented somites. At first, we examined the expression of *Mesp1*, which was neighboring and structurally related to *Mesp2* and expressed in the identical region with *Mesp2* during somitogenesis. In the *Mesp2* (−/−) embryos, *Mesp1* expression was observed at an almost identical site with the wild-type embryos (Fig. 8A). This result suggests that mesenchymal cells expected to express *Mesp2* were present at the appropriate region in *Mesp2* (−/−) embryos.

Notch1, *Notch2*, and *Dll1* are expressed predominantly at the presomitic mesoderm and are involved in epithelialization of the mesenchymal cells and segmentation of the somite (Bettenhausen et al. 1995; Conlon et al. 1995; Williams et al. 1995; Hrabe de Angelis et al. 1997). In the 9.5-dpc wild-type embryos, *Notch1* and *Dll1* mRNA expression were compared with *Mesp2* by two-color whole mount in situ hybridization. *Notch1* mRNA was expressed in the presomitic mesoderm, including the anterior end that was about to form a new somite, whereas *Mesp2* mRNA was localized to a part of the *Notch1*-expressing mesoderm just one somite-length

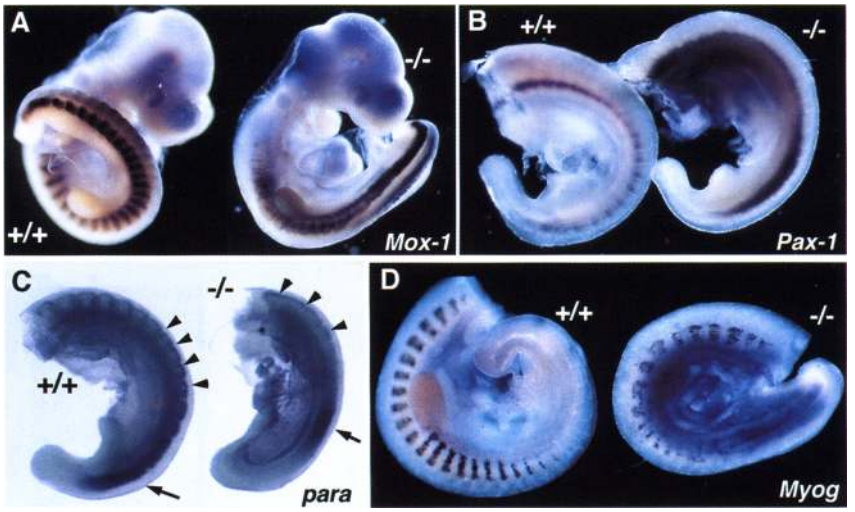

Figure 7. Analysis of somitic mesodermal markers in *Mesp2* (−/−) embryos by whole mount in situ hybridization. The probes used were *Mox-1* (*A*), *Pax-1* (*B*), *Paraxis* (*C*), and *Myog* (*D*). *Paraxis* was expressed initially in the rostral part of the presomitic mesoderm and in newly formed somites (indicated by arrows in *C*) and was localized in the dermatome with differentiation (arrowheads). The embryo samples used were prepared at 9.5 dpc.

posterior to its anterior end (Fig. 8B). The anterior end of *Dll1* mRNA expression was found to overlap with that of *Mesp2* (Fig. 8C).

In the *Mesp2* (−/−) embryos, both *Notch1* and *Notch2* were markedly affected. The *Notch1* signal was observed in the mature somite and neural tube in addition to its predominant expression in presomitic mesoderm in the wild-type embryos. However, only lower levels of expression were detected in either presumptive somite or presomitic mesoderm of *Mesp2* (−/−) embryos (Fig. 8D). *Notch2* was expressed in the anterior part of presomitic mesoderm and rostral half of newly segmented somite in wild-type embryos; however, the expression was not detected in *Mesp2* (−/−) embryos (Fig. 8E). In contrast, *Dll1* expression was not reduced in the presumptive presomitic mesoderm despite the lack of segmentation in the *Mesp2* (−/−) embryos (Fig. 8F). More cranially, *Dll1* showed a uniform expression in *Mesp2* (−/−) embryos, whereas *Dll1* was expressed predominantly in the caudal region of each somite in the wild-type embryos (Fig. 8F). This is probably attributable to the lack of the segmentation and segment polarity of the somitic mesoderm. These results indicate that MesP2 plays an important role in somitogenesis by regulating the notch–delta signaling system.

Another signaling pathway that acts through the

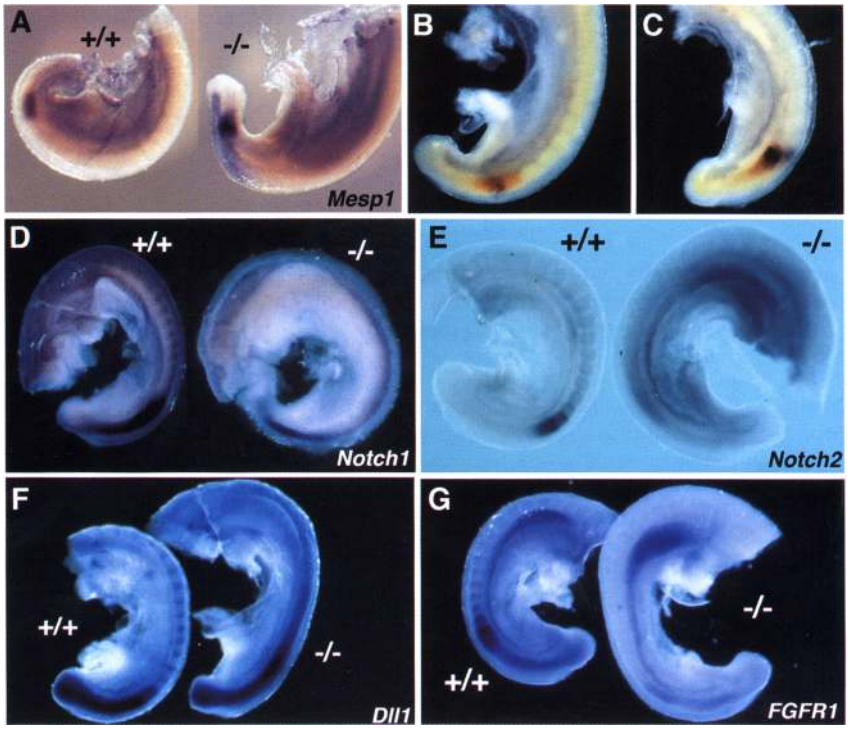

Figure 8. Comparison of genetic activity in presomitic mesoderm in wild-type and *Mesp2* (−/−) embryos. The probes used were *Mesp1* (*A*), *Notch1* (*D*), *Notch2* (*E*), *Dll1* (*F*), and *FGFR1* (*G*). (*B*,*C*) Double staining analyses of the expression domains for *Mesp2* and *Notch1* (*B*) and for *Mesp2* and *Dll1* (*C*) in the wild-type embryo. The orange color represents *Notch1* (*B*) and *Dll1* (*C*), respectively, and the purple color represents the *Mesp2* expression domain (*B*,*C*). The embryo samples were prepared at 9.5 dpc. Only the caudal or tail region is shown.

FGFR1 protein has also been implicated in the normal formation of somites (Deng et al. 1994; Yamaguchi et al. 1994). Therefore, we analyzed the expression of *FGFR1* in *Mesp2* (-/-) embryos to see if this pathway was affected by the mutation. The expression of the *FGFR1* gene marks the anterior portion of the presomitic mesoderm and the newly formed somite in the wild-type embryos. Interestingly, *FGFR1* was not expressed in the presomitic mesoderm of *Mesp2* (-/-) embryos, although its expression in the limb bud region was not affected (Fig. 8G). This clearly indicates that MesP2 regulates the FGF signaling pathway in addition to the notch–delta signaling pathway.

Discussion

In this study, we isolated a new member of the bHLH gene family, *Mesp2*, which is expressed in the rostral region of the presomitic mesoderm one segment-width from the boundary between the presomitic mesoderm and the segmenting somite and that overlaps with the expression domain of a closely related gene *Mesp1*. Targeted disruption of *Mesp2* impairs budding of the spherical somite from the unsegmented paraxial mesoderm, and consequently leads to extensive fusion of the vertebral column.

Mesp2 *is required to establish the rostrocaudal segment polarity of somites*

The results obtained from the analysis of the *Mesp2* (-/-) mice indicate that the *Mesp2* gene product is indispensable for the development of sclerotomal polarity. First, segmentation of the axial skeleton was severely disturbed along the entire axis in newborn *Mesp2* (-/-) mice, except in the craniofacial region. The pedicles of the neural arches, the lateral processes of the vertebrae, and the proximal parts of the ribs were fused completely. Because these structures are thought to be derived from the posterior half of the epithelial somites or somitocoel cells, this phenomenon suggests that *Mesp2* (-/-) mutants lack the properties of the anterior half of the sclerotome, resulting in the expansion of posterior sclerotomal characteristics into the anterior halves by misspecification or respecification of characteristics and the properties of the rostral sclerotomal halves (Stern and Keynes 1987; Goldstein and Kaleheim 1992). Second, both *Mox-1* and *Pax-1* expression, which demarcates the posterior half of the sclerotome (Koseki et al. 1993), was enhanced in the entire sclerotome, and the metameric pattern of their expression domains was lost completely in the *Mesp2* (-/-) embryos. In addition, *Dll1* expression, which was shown to be localized in the caudal part of the sclerotome and to be involved in the maintenance of sclerotome polarity (Hrabe de Angelis et al. 1997), was expanded in the *Mesp2* (-/-) mutant embryos (Fig. 8F). These observations again suggest the expansion of the posterior half of the sclerotome. Finally, the anomalous development of DRG also suggests functional impairment of the anterior sclerotome derivatives. In the *Mesp2* (-/-) mice, the DRG were less developed, particularly in the trunk region, were located more dorsally than in the wild-type embryos, and were fused together with poorly developed septa. Axonal outgrowth of peripheral nerves was also inhibited strongly. Similar consequences regarding DRG development were reported in manipulated chick embryos that had multiple caudal half somites from quail embryos (Kalcheim and Teillet 1989). Because neural crest cells migrate exclusively into the rostral region of the sclerotome and peripheral nerve axons pass through the cranioventral region of the sclerotome (Bronner-Fraser 1986; Loring and Erickson 1987), lack of the properties of the rostral half of the developing sclerotome is again indicated in *Mesp2* (-/-) mice.

Interestingly, the earliest prominent phenotype of *Mesp2* (-/-) embryos was a lack of initial somite segmentation. Although the expression of *Mesp1*, which overlaps completely with the *Mesp2* expression domain in the rostral region of the unsegmented mesoderm, appears at an appropriate distance from the tail bud in the *Mesp2* (-/-) mice, budding of the epithelial somites was not seen in this region. Thus, transition between the presomitic mesoderm and the epithelial somite at the proper position requires the presence of MesP2 protein. Therefore, lack of the properties of the anterior half of the somite in the paraxial mesoderm and lack of somite segmentation might be tightly coupled in the *Mesp2* (-/-) mutant. Previously, the rostrocaudal subdivision was suggested to be required to maintain the segmental arrangement of the chick paraxial mesoderm (Stern and Keynes 1986). A transplantation experiment in chick embryos clearly demonstrated that rostrocaudal polarity is generated at the segmentation stage (Keynes and Stern 1988). *Mesp2* is only expressed in the presomitic mesoderm just before segmentation (at least the transcript). Thus, it is probable that MesP2 functions to establish initial rostrocaudal polarity and is not involved in its maintenance. However, there is no appropriate marker to define rostrocaudal polarity in the presomitic mesoderm. At this point, we cannot exclude the possibility that rostrocaudal polarity is established in the presomitic mesoderm initially, and is lost during subsequent development in *Mesp2* (-/-) mutants.

Segmentation in Mesp2 *(-/-) mutants*

Although somite segmentation is strongly impaired in *Mesp2* (-/-) mutants, apparently segmented features were retained in the distal part of the ribs and in the developing myotome as shown by *Myog* expression. Detailed histological analysis revealed that somitogenesis in the *Mesp2* (-/-) mutants occurred in an abnormal sequence. First, spherical tight cell aggregates were never generated, but dermomyotome differentiation followed without segmentation. Then, dermomyotomal segmentation preceded sclerotomal segmentation. Finally, sclerotomal segmentation was observed without rosto-

caudal polarity. It has been suggested that the periodicity of somite segmentation is prepatterned in the presomitic mesoderm as a serially repeated radial arrangement of somitomeres (Meier 1979). It is conceivable that this predetermined state is retained in the developing paraxial mesoderm without overt segmentation in *Mesp2* (−/−) mutants and that the intrinsic periodicity of the paraxial mesoderm appears much later. Thus, *Mesp2* might be essential for the coordinate segmentation of the somite but not for the generation of periodicity of the paraxial mesoderm.

A strong correlation between somite segmentation and the cell division cycle of the paraxial mesoderm was proposed by Primmett et al. (1988, 1989). They observed an abnormal periodic appearance of somites, mainly fusion of two consecutive somites after a single episode of heat shock or treatment with cell cycle inhibitors. Thus, the periodicity of the paraxial mesoderm was suggested to be dependent on the synchronicity of the cell cycle of the somitic stem cells. Interestingly, Primmett et al. observed a lack or defect of the anterior half of sclerotomes in the affected regions, exhibiting a resemblance to *Mesp2* phenotypes. Thus, it is possible that *Mesp2* expression itself or condensation of *Mesp2*-expressing cells in the segmental plate is influenced by the progression of the cell cycle of somitic mesoderm stem cells.

Intriguingly, the generation of basi-, exo-, and supraoccipital bones and occipitoatlantic joints remained intact in *Mesp2* (−/−) mice. This is in agreement with the observation that the most rostral somites 2–5 fuse to generate an occipital bone (Christ and Wilting 1992), which may indicate a natural lack of the rostral part in these somites. Thus, the *Mesp2* gene product is not essential for segmentation of the occipital somites, and it is possible that a separate gene is responsible for this process. A structurally related and neighboring gene, MesP1, may be involved in somitogenesis in the presumptive occipital region. Although MesP1 cannot compensate fully for MesP2 function in the trunk region, these two gene products possess 93% amino acid identity in the bHLH region and their expression domains overlap completely during somite segmentation.

Mesp2 *functions through the notch–delta and FGF signaling pathway*

Recently, it was suggested that the notch-delta signaling pathway is involved in somitogenesis (Artavanis-Tsakonas et al. 1995). In *Notch1*-deficient mice, a delay and a lack of coordination in the segmentation of somites were observed (Conlon et al. 1995). Mice deficient in *RBP-Jk* gene product, a homolog of the *Drosophila* suppressor of Hairless [*Su(H)*], which functions in the downstream of the notch–signal–transducing cascade, also exhibited a similar phenotype in the paraxial mesoderm (Oka et al. 1995). Recently, a vertebrate homolog of delta, *Dll1*, was found to be expressed in the presomitic paraxial mesoderm and subsequently in the posterior halves of somites (Bettenhausen et al. 1995). Inactivation of the *Dll1* locus leads to defective segmentation that is probably induced by the loss of the properties of the posterior half of the somites (Hrabe de Angelis et al. 1997). Therefore, it is possible that a balanced interaction between the mammalian homologs of notch and delta molecules plays a crucial role during the transition from presegmented mesoderm to somite. In *Mesp2* mutants, both *Notch1* and *Notch2* expression was decreased significantly, whereas *Dll1* expression was not affected. Thus, the expression of *Notch* genes is under the control of *Mesp2* gene product. The notch–delta signaling pathway is known to have an essential role in the establishment of boundaries between two adjacent distinct territories in both invertebrates and vertebrates (Ma et al. 1996). Recently, molecular circuitry including bHLH gene, *Xenopus Neurogenin*-related (*XNGNR-1*), *X-Notch-1*, and *X-Delta-1* is indicated to be required for the lateral inhibition and neuronal determination of *Xenopus* embryos. Here, *XNGNR-1* expression is regulated negatively by signals from activated *X-Notch* receptor and *XNGNR-1* gene products induce the expression of *X-Delta-1*. Eventually, this molecular circuitry allows for the generation of a boundary between territories solely expressing *X-Notch-1* or *X-Delta-1*. Our comparative analyses of the expression of *Mesp2*, *Notch1*, *Notch2*, and *Dll1* in 9.5-dpc embryos indicates a sequential gene activation during the maturation of the presomitic mesoderm, suggesting the presence of similar molecular circuitry during segmentation and the establishment of polarity of the paraxial mesoderm, although the analyses were limited only to RNA (Fig. 9).

It is worth noting that *Notch1* was expressed in a much wider region than was *Mesp2*, and that *Notch1* expression in the more caudal presomitic mesoderm was

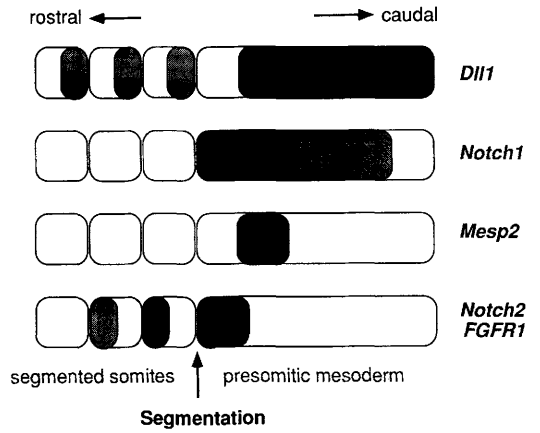

Figure 9. Schematic presentation of gene activities in presomitic mesoderm. The presomitic mesoderm is composed of discrete domains characterized by differential expression of *Mesp2*, *Notch1*, *Notch2*, *Dll1*, and *FGFR1*. Before somite formation, *Dll1* may be activated first, followed by *Notch1*. *Mesp2* expression induces high and localized expression of *Notch1*, which may result in the down-regulation of *Dll1* and activation of *Notch2*. The newly formed somite was polarized by the differential expression of *Notch2* (and *FGFR1*) in the rostral half and *Dll1* in the caudal half.

affected in *Mesp2* (-/-) embryos. This indicates the existence of nonautonomous effects of MesP2 for *Notch1* expression in the presomitic mesoderm rather than simple transcriptional activation.

Interestingly, although the phenotypes of the *Mesp2* (-/-) and *Notch1* mutants resemble each other in the somitic mesoderm stage, the *Mesp2* (-/-) mouse has a more severely affected phenotype than the *Notch1*-deficient mouse. It is worth noting that the expression of *FGFR1*, which was not affected in the *Notch1* (-/-) mutants (Conlon et al. 1995), was also reduced in the *Mesp2* (-/-) mutants. The notable similarity in the expression pattern between *Notch2* and *FGFR1* and the positive regulation by MesP2, suggests a relationship between the two signaling systems mediated by notch-delta and FGF. Alternatively, however, these systems may be regulated independently but simultaneously by MesP2.

Genetic cascades involved in the epithelial somite formation

Recent genetic evidence together with the finding of the present study suggest that epithelial somite formation can be divided into at least two distinct phases. The first phase is the segmentation of the paraxial mesoderm, in which the notch-delta system plays a pivotal role. The second phase is the epithelial condensation of the mesenchymal presomitic mesoderm, in which *paraxis* gene product is indispensable. The expression of *paraxis* at the appropriate position in the *Mesp2* (-/-) embryos suggests that segmentation of the paraxial mesoderm is not required for the subsequent expression of *paraxis*. Thus, it is conceivable that the expression of *Mesp2* and *paraxis*, which represent segmentation and epithelialization, respectively, are controlled independently. However, we cannot exclude the possibility that there is no initial epithelialization in *Mesp2* (-/-) mutants in addition to the lack of segmentation, because there is no good molecular marker to demonstrate epithelialization upon segmentation. Morphological changes in cell shape and compaction are the only markers for the initial epithelialization. More detailed investigation will be required to confirm initial epithelialization in *Mesp2* (-/-) mutants.

In the mouse, several classic mutants were suggested to result from defects in somite segmentation (Theiler et al. 1975; Hogan et al. 1985). Skeletal anomalies similar to those of *Mesp2* (-/-) mutants are seen in *Rib fusions* (*Rf*), *Malformed vertebrae* (*Mv*), *pudgy* (*pu*), and *amputated* (*am*). In *Rf*, *Mv*, and *pu* mutants, fusion of somites is thought to cause the abnormal vertebral column development. It is possible that *Mesp2* (-/-) is allelic for *Rf*, *Mv*, and *pu* mutations, although there are several phenotypic differences. Alternatively, gene products encoded by *Rf*, *Mv*, and *pu* loci may be involved in the notch–delta signaling pathway. Therefore, genetic and molecular analysis of these mutants in relation to *Mesp2* and the notch–delta signaling system can provide further insight on the mechanism leading to somitic segmentation.

Materials and methods

Cloning of the Mesp2 *gene*

The *Mesp2* gene was isolated from a TT2 embryonic stem (ES) cell genomic library by cross-hybridization with the *Mesp1* cDNA probe. Complementary DNA for *Mesp2* was then isolated by the hybrid capture method from PCR-amplified 8.5-dpc cDNA (Abe 1992) using a genomic DNA fragment as a probe. The detailed method for hybrid capture was described as RARGIP (random access retrieval of genetic information through PCR) (Abe 1992). Because the cDNA lacked the 5′ region, its sequence was determined by analyzing the genomic DNA (Fig. 1B) using either Sequenase II (U.S. Biochemical) or in a Perkin-Elmer model ABI377 sequencer, and analyzed using a GCG sequence analysis software package.

Vector construction and homologous recombination

Genomic clone GD-12 for the mouse *Mesp2* genes were isolated from a TT2 ES cell genomic DNA library established in λ *Fix*II by a cross-hybridization with a *Mesp1* cDNA probe. To construct the targeting vector, an 6-kb DNA fragment spanning from the *Eco*RI to the *Bam*HI site in the 5′ upstream region of exon 1 was subcloned into Bluescript (SK+) to make EB-6.0. A phosphoglycerokinase (pgk)-neomycin (neo) cassette was ligated with the EB-6.0 to generate EB-6.0–neo. For the short homology arm, a 1-kb fragment spanning from the *Xba*I site downstream of exon-2 to the 3′ end of GD-12 was isolated and ligated with the pgk–DT–A cassette to construct X1.0–DT–A. The fragment containing X1.0–DT–A was ligated with EB-6.0–neo to construct *Mesp2* targeting vector (Fig. 3A). This vector was linearized at the *Not*I site and electroporated into TT2 ES cells [C57BL/6 (B6)/CBA] as described previously (Yagi et al. 1993). After selection with G418, resistant clones were picked up and their DNAs were analyzed by PCR using a neo-specific primer NeoAL, and a *Mesp2* genomic primer GR3. The sequences for these primers were (NeoAL) 5′-GAAAGAACCAGCTGGGGCTCGAG-3′ and (*Mesp2*–GR3) 5′-GGAAGTTGAGTTCCTCATCACGATC-3′, respectively. Of 201 G418-resistant ES cell clones, four homologous recombinant clones were selected by PCR and verified by Southern blot analysis (Fig. 3B). Clones 59 and 84 were injected into ICR mouse 8-cell embryos and germ line chimera were obtained from both clones.

Generation of chimeras and genotyping of wild-type and mutant alleles

Embryo manipulations and injection of the ES cell clones into ICR 8-cell embryos were carried out as described (Yagi et al. 1993). Chimeric mice with a high contribution of TT2 genetic background (monitored by agouti coat color) were bred either with C57BL/6 or ICR mice. Genotypes of embryo mice were assessed routinely by PCR analyses with genomic DNA prepared from yolk sac. The wild-type allele was detected as the 319-bp product with primers *Mesp2*-L3 and *Mesp2*-R3. The sequences for these primers were *Mesp2*-L3, 5′-CATCATGCCAGAGACTACAGCCTCA-3′, and *Mesp2*-R3, 5′-GTCACGGCATTAGCAAGGTTGAGAA-3′, respectively.

Embryo analysis by whole mount in situ hybridization or whole mount immunohistostaining

The following anti-sense probes were prepared from *Mesp1* and *Mesp2* cDNA. Probe MesP1, the original PB92 cDNA clone digested with *Xho*I to remove the bHLH region (Saga et al. 1996). Probe MesP2, cDNA clone linearized with *Bam*HI site within

exon 1 to remove the bHLH region. The method for the whole mount in situ hybridization was described before (Saga et al. 1996). For double in situ hybridization, fluorescein isothiocyanate (FITC)-labeled RNA probe was detected by anti-FITC AP conjugate and the orange color was developed in INT-BCIP solution (Boehringer Mannheim). The method for immunohistostaining using monoclonal antibody 2H3 (Developmental studies hybridoma bank) was described (Matsuo et al. 1995).

Skeletal analysis

Cartilages and bones were stained with alcian blue and alizarin red by the following method. After removing skin and viscera, animal was fixed in 95% ethanol for 5 days and in acetone for 2 days, and stained in 0.3% alcian blue in 70% ethanol/0.1% alizarin red in 95% ethanol/acetic acid/70% ethanol (1:1:1:17) for 12 hr. After washing with distilled water, specimens were placed in 1% KOH for 24–48 hr and cleared by incubation in 20%, 50%, and 80% glycerol steps.

Acknowledgments

We are grateful to Alvert F. Candia, Ron Conlon, Domingos Henrique, Alan Rawel for the gift of the *Mox-1*, *Notch1*, *Dll1*, and *paraxis* cDNA clones, respectively. We are also grateful to Achim Gossler for communicating the unpublished data, to Shigeru Kuratani for many valuable discussion, and to Claudio D. Stern for critical reading of the manuscript. This research was supported partly by TARA project (University of Tsukuba, Japan).

The publication costs of this article were defrayed in part by payment of page charges. This article must therefore be hereby marked "advertisement" in accordance with 18 USC section 1734 solely to indicate this fact.

Note

The sequence data for *Mesp2* cDNA has been deposited in GenBank under accession no. U71125.

References

Abe, K. 1992. Rapid isolation of desired sequences from lone linker PCR amplified cDNA mixtures: Application to identification and recovery of expressed sequences in cloned genomic DNA. *Mamm. Genome* **2:** 252–259.

Aoyama, H. and K. Asamoto. 1988. Determination of somite cells: Independence of cell differentiation and morphogenesis. *Development* **104:** 15–28.

Artavanis-Tsakonas, S., K. Matsuno, and M.E. Fortini. 1995. Notch signaling. *Science* **268:** 225–232.

Bettenhausen, B., M. Hrabe de Angelis, D. Simon, J.L. Guenet, and A. Gossler. 1995. Transient and restricted expression during mouse embryogenesis of *Dll1*, a murine gene closely related to Drosophila Delta. *Development* **121:** 2407–2418.

Bronner-Fraser, M. 1986. Analysis of the early stages of trunk neural crest cell migration in avian embryos using monoclonal antibody HNK-1. *Dev. Biol.* **115:** 44–55.

Burgess, R., P. Cserjesi, K. Ligon, and E.N. Olson. 1995. Paraxis: A basic helix–loop–helix protein expressed in paraxial mesoderm and developing somites. *Dev. Biol.* **168:** 296–306.

Burgess, R., A. Rawls, D. Brown, A. Bradley, and E.N. Olson. 1996. Requirement of the *paraxis* gene for somite formation and musculoskeletal patterning. *Nature* **384:** 570–573.

Cai, M. and R.W. Davis. 1990. Yeast centromere binding protein CBF1, of the helix–loop–helix protein family, is required for chromosome stability and methionine prototrophy. *Cell* **61:** 437–446.

Candia, A.F., J. Hu, J. Crosby, P.A. Lalley, D. Noden, J.H. Nadeau, and C.V.E. Wright. 1992. *Mox-1* and *Mox-2* define a novel homeobox gene subfamily and are differentially expressed during early mesodermal patterning in mouse embryos. *Development* **116:** 1123–1136.

Christ, B. and J. Wilting. 1992. From somites to vertebral column. *Ann. Anat.* **174:** 23–32.

Conlon, R.A., A.G. Reaume, and J. Rossant. 1995. *Notch1* is required for the coordinate segmentation of somites. *Development* **121:** 1533–1545.

Deng, C.-X., A. Wynshaw-Boris, M.M. Shen, C. Daugherty, D.M. Ornitx, and P. Leder. 1994. Murine FGFR-1 is required for early postimplantation growth and axial organization. *Genes & Dev.* **8:** 3045–3057.

Edmondson, D.G. and E.N. Olson. 1989. A gene with homology to the *myc* similarity region of *MyoD1* is expressed during myogenesis and is sufficient to activate the muscle differentiation program. *Genes & Dev.* **3:** 628–640.

Goldstein, R.S. and C. Kalcheim. 1992. Determination of epithelial half-somites in skeletal morphogenesis. *Development* **116:** 441–445.

Hrabe de Angelis, M., J. McIntyre II, and A. Gossler. 1997. Maintenance of somite borders in mice requires the *Delta* homologue *Dll1*. *Nature* **386:** 717–721.

Hogan, B., P. Holland, and P. Schofield. 1985. How is the mouse segmented? *Trends Genet.* **1:** 67–74.

Kalcheim, C. and M.-A. Teillet. 1989. Consequences of somite manipulation on the pattern of dorsal root ganglion development. *Development* **106:** 85–93.

Keynes, R. and C.D. Stern. 1988. Mechanisms of vertebrate segmentation. *Development* **103:** 413–429.

Koseki, H., J. Wallin, J. Wilting, Y. Mizutani, A. Kispert, C. Ebensperger, B.G. Herrmann, B. Christ, and R. Balling. 1993. A role for Pax-1 as a mediator of notochordal signals during the dorsoventral specification of vertebrae. *Development* **119:** 649–660.

Loring, J. and C. Erickson. 1987. Neural crest cell migration pathways in the chick embryo. *Dev. Biol.* **121:** 230–236.

Ma, Q., C. Kintner, and D.J. Anderson. 1996. Identification of *neurogenin*, a vertebrate neuronal determination gene. *Cell* **87:** 43–52.

Matsuo, I., S. Kuratani, C. Kimura, N. Takeda, and S. Aizawa. 1995. Mouse Otx2 functions in the formation and patterning of rostral head. *Genes & Dev.* **9:** 2646–2658.

Meier, S. 1979. Development of the chick mesoblast. Formation of embryonic axis and establishment of the metameric pattern. *Dev. Biol.* **73:** 25–45.

Oka, C., T. Nakano, A. Wakehan, J.L. de ka Oinoa, C. Mori, T. Sakai, S. Okawaki, M. Kawaichi, K. Shiota, T.W. Mak, and T. Honjo. 1995. Disruption of the mouse RBP-Jk gene results in early embryonic death. *Development* **121:** 3291–3301.

Ostrovsky, D., J. Sanger, and J.W. Lash. 1988. Somitogenesis in the mouse embryo. *Cell Differ.* **23:** 17–26.

Primmett, D.R.N., C.D. Stern, and R.J. Keynes. 1988. Heat shock causes repeated segmental anomalies in the chick embryo. *Development* **104:** 331–339.

Primmett, D.R.N., W. Norris, G. Carlson, R.J. Keynes, and C.D. Stern. 1989. Periodic segmental anomalies induced by heat-shock in the chick embryo are associated with the cell cycle. *Development* **105:** 119–130.

Quertermous, E.E., H. Hidai, M.A. Blanar, and T. Quertermous. 1994. Cloning and characterization of a basic helix–loop–helix protein expressed in the early mesoderm and the de-

veloping somites. *Proc. Natl. Acad. Sci.* **91:** 7066–7070.

Rickmann, M., J.W. Fawcett, and R.J. Keyners. 1985. The migration of neural crest cells and the growth of motor axons through the rostral half of the chick somite. *J. Embryol. Exp. Morphol.* **90:** 437–455.

Saga, Y., N. Hata, S. Kobayashi, T. Magnuson, M. Seldin, and M.M. Taketo. 1996. MesP1: A novel basic helix–loop–helix protein expressed in the nascent mesodermal cells during mouse gastrulation. *Development* **122:** 2769–2778.

Stern, C.D. and R.J. Keynes. 1986. Cell lineage and the formation and maintenance of half somites. In *Somites in developing embryo* (ed. R. Bellairs, D.A. Ede, and J.W. Lash), pp. 147–159. Plenum Press, New York, NY.

———. 1987. Interactions between somite cells: The formation and maintenance of segment boundaries in the chick embryo. *Development* **99:** 261–272.

Stern, C.D., S.M. Sisodiya, and R.J. Keynes. 1986. Interactions between somite cells: Inhibition and stimulation of nerve growth in the chick embryo. *J. Embryol. Exp. Morphol.* **91:** 209–226.

Swiatek, P.J., C.E. Lindsell, F.F. del Amo, G. Weinmaster, and T. Gridley. 1994. *Notch1* is essential for postimplantation development in mice. *Genes & Dev.* **8:** 707–719.

Tam, P.P.L. and P.A. Trainor. 1994. Specification and segmentation of the paraxial mesoderm. *Anat. Embryol.* **189:** 275–305.

Theiler, K., D.S. Varnum, J.L. Southard, and L.C. Stevens. 1975. *Malformed vertebrae:* A new mutant with the "wirbel-rippen syndrom" in the mouse. *Anat. Embryol.* **147:** 161–166.

Williams, R., U. Lendahl, and M. Lardelli. 1995. Complementary and combinatorial patterns of Notch gene family expression during early mouse development. *Mech. Dev.* **53:** 357–368.

Yagi, T., T. Tokunaga, Y. Furuta, S. Nada, M. Yoshida, T. Tsukada, Y. Saga, N. Takeda, Y. Ikawa, and S. Aizawa. 1993. A novel ES cell line, TT2, with high germline-differentiating potency. *Analyt. Biochem.* **214:** 70–76.

Yamaguchi, T.P., R.A. Conlon, and J. Rossant. 1992. Expression of the fibroblast growth factor receptor FGFR-1/flg during gastrulation and segmentation in the mouse embryo. *Dev. Biol.* **152:** 75–88.

Yamaguchi, T.P., K. Harpal, M. Henkemeyer, and J. Rossant. 1994. *fgfr-1* is required for embryonic growth and mesodermal patterning during mouse gastrulation. *Genes & Dev.* **8:** 3032–3044

Mesp2: a novel mouse gene expressed in the presegmented mesoderm and essential for segmentation initiation.

Y Saga, N Hata, H Koseki, et al.

Genes Dev. 1997, **11:**
Access the most recent version at doi:10.1101/gad.11.14.1827